

4. T. Chao-Hsiung and C. Chih-Lin, Improvement of return loss bandwidth of balanced amplifier using metamaterial-based quadrature power splitters, *IEEE Microwave Wireless Compon Lett* 18 (2008), 269–271.
5. M.A. Antoniadis and G.V. Eleftheriades, A broadband Wilkinson balun using microstrip metamaterial lines, *IEEE Antennas Wireless Propag Lett* 4 (2005), 209–212.
6. N. Seman and M. Bialkowski, Microstrip-slot transition and its applications in multilayer microwave circuits, In: V. Zhurbenko (Ed.), *Passive microwave components and antennas*, IN-TECH, Austria, 2010, pp. 247–266.
7. A.M. Abbosh, Ultra-wideband phase shifters, *IEEE Microwave Theory Tech* 55 (2007), 1935–1941.
8. A.M. Abbosh, Broadband fixed phase shifters, *IEEE Microwave Wireless Compon Lett* 21 (2011), 22–24.

© 2011 Wiley Periodicals, Inc.

## BANDWIDTH ENHANCEMENT OF WWAN/LTE TABLET COMPUTER ANTENNA USING EMBEDDED PARALLEL RESONANT CIRCUIT

Kin-Lu Wong,<sup>1</sup> Ying-Chien Liu,<sup>1</sup> and Liang-Che Chou<sup>2</sup>

<sup>1</sup> Department of Electrical Engineering, National Sun Yat-Sen University, Kaohsiung 804, Taiwan; Corresponding author: wongkl@ema.ee.nsysu.edu.tw

<sup>2</sup> Department of High Frequency Business, Yageo Corporation Nantze Branch, Kaohsiung 811, Taiwan

Received 7 May 2011

**ABSTRACT:** By embedding a printed parallel resonant circuit, the lower-band bandwidth of the proposed internal tablet computer antenna is greatly enhanced. This bandwidth-enhancement technique allows the proposed antenna to cover the eight-band wireless wide area network/long term evolution operation in the 704–960 and 1710–2690 MHz bands with a small size of  $12 \times 60 \times 3.8 \text{ mm}^3$  in the tablet computer. The main radiator of the antenna comprises a patch monopole, a longer shorted strip, and a shorter shorted strip. The latter two shorted strips form the outer boundary of the antenna and are parasitically excited by the patch monopole. The parallel resonant circuit is formed by embedding a chip-inductor-loaded narrow strip in-between the longer shorted strip and the patch monopole, with the narrow strip whose front terminal connected to the patch monopole and end section gap-coupled to the longer shorted strip. This embedded circuit can lead to the generation of a parallel resonance seen at the antenna's feeding point. By controlling the parallel resonance to be at the high-frequency tail of the resonant mode at about 800 MHz contributed by the longer shorted strip, an additional resonance can be generated, which can result in dual-resonance excitation of the original single-resonance mode. Thus, a wide antenna's lower band is obtained. Further, the patch monopole can contribute a resonant mode to combine additional resonant modes contributed by the two shorted strips to form a wide antenna's upper band. Details of the proposed antenna with the embedded parallel resonant circuit are described in the article. © 2011 Wiley Periodicals, Inc. *Microwave Opt Technol Lett* 54:305–309, 2012; View this article online at [wileyonlinelibrary.com](http://wileyonlinelibrary.com). DOI 10.1002/mop.26580

**Key words:** mobile antennas; tablet computer antennas; WWAN antennas; LTE antennas; embedded parallel resonant circuit

### 1. INTRODUCTION

The occupied size of the internal laptop computer or tablet computer antennas for the penta-band wireless wide area network (WWAN) or eight-band WWAN/long term evolution (LTE)

operation is generally not easy to be reduced owing to the large lower-band bandwidth required (for instance, 824–960 MHz for the GSM850/900 operation or 704–960 MHz for the LTE700/GSM850/900 operation) [1–12]. The requirement of large lower-band bandwidth is especially more challenging for the internal antenna in the tablet computer than in the mobile handset. This is because the size of the system ground plane is generally much larger in the tablet computer than in the mobile handset [13–16], thus making the chassis mode of the system ground plane generally cannot be excited to assist in achieving a wider lower band for the embedded internal antenna.

To overcome the aforementioned problem for the internal WWAN/LTE antenna embedded in the tablet computer, we present a bandwidth-enhancement technique by using a distributed parallel resonant circuit embedded in the antenna, which does not increase the antenna's occupied size and can lead to a dual-resonance excitation of the antenna's lower band for the LTE700/GSM850/900 (704–960 MHz) operation with a small size of  $12 \times 60 \times 3.8 \text{ mm}^3$ . The distributed parallel resonant circuit is obtained by embedding a long narrow strip with its front terminal connected to one part of the antenna's main radiator and its end section gap-coupled to the other part of the main radiator. The former provides an additional inductance and the latter contributes an equivalent capacitance, and both can lead to the generation of a parallel resonance seen at the antenna's feeding point [17]. This parallel resonance can result in the generation of an additional resonance at the high-frequency tail of the original single-resonance mode in the antenna's lower band, such that the original single-resonance mode can become a dual-resonance mode to provide a much wider lower-band bandwidth for the antenna. Note that as the embedded parallel resonant circuit does not increase the occupied size of the antenna, bandwidth enhancement is obtained without a sacrifice in increasing the antenna size.

Further, the antenna can provide a wide upper band for the GSM1800/1900/UMTS/LTE2300/2500 (1710–2690 MHz) operation. That is, the proposed antenna can cover the eight-band WWAN/LTE operation with an occupied size about the smallest among the related reported antenna for tablet computer or laptop computer applications [11, 14–16]. Details of the proposed antenna and the operating principle of the embedded parallel resonant circuit are described in the article. The antenna was fabricated and tested. Results of the fabricated antenna are presented and discussed.

### 2. PROPOSED ANTENNA

Figure 1 shows the geometry of the proposed WWAN/LTE tablet computer antenna with an embedded parallel resonant circuit. A photo of the fabricated antenna is shown in Figure 2. The antenna is formed by two portions. The first portion is printed on a 0.8-mm thick FR4 substrate of relative permittivity 4.4, loss tangent 0.02, and size  $12 \times 60 \text{ mm}^2$ , and the second portion is a metal strip of width 3 mm and length 60 mm ( $t$  in the figure) cut from a 0.2-mm thick copper plate. The second portion is oriented perpendicular to and connected with the first portion as shown in the figure. In this study, the antenna is to be applied in a 9.7-inch tablet computer, which is currently commercially available. The antenna is mounted along the edge of the top shielding metal wall ( $5 \times 150 \text{ mm}^2$ ) of the display ground ( $150 \times 200 \text{ mm}^2$ ), which is used to support a 9.7-inch display. Note that the antenna is placed close to one corner of the shielding metal wall such that other possible internal antennas (for instance, the WLAN antenna, the multiple-input multiple-output antenna system [18], etc.) can also be mounted along the

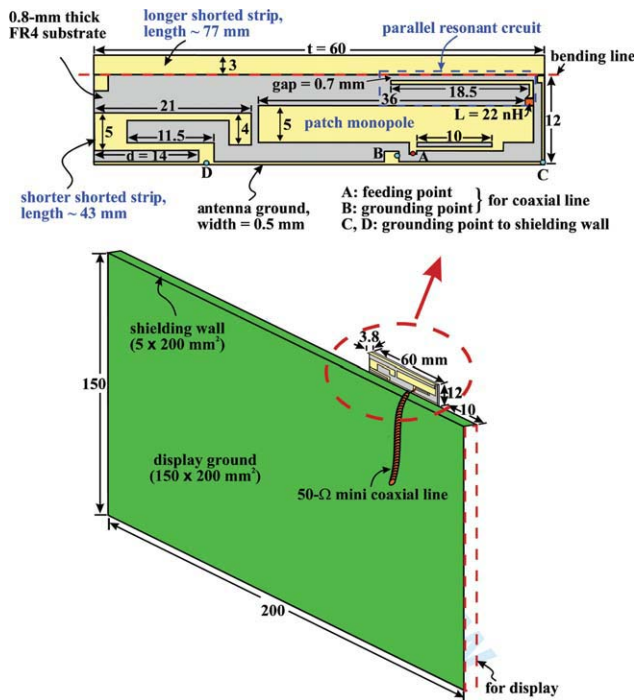


**Figure 1** Geometry of the proposed WWAN/LTE tablet computer antenna with an embedded parallel resonant circuit. [Color figure can be viewed in the online issue, which is available at [wileyonlinelibrary.com](http://wileyonlinelibrary.com)]

shielding metal wall to achieve efficient integration of the internal antennas in the tablet computer.

The antenna comprises a main radiator and an antenna ground. The antenna ground has a narrow width of 0.5 mm and a length of 60 mm and is disposed at the bottom edge of the antenna. The antenna ground is connected at points C and D to the shielding metal wall for testing the antenna in the experiment in this study. The antenna is fed by a 50- $\Omega$  mini coaxial line, whose grounding sheath is connected to point B at the small grounding pad of the antenna ground and central connector is connected to point A, the feeding point of the antenna. The antenna's main radiator mainly comprises a patch monopole, a longer shorted strip, and a shorter shorted strip. The latter two shorted strips are parasitically excited. The longer shorted strip having a length of about 77 mm can generate a quarter-wavelength resonant mode in the antenna's desired lower band and a higher-order resonant mode in the desired upper band. The shorter shorted strip having a length of about 43 mm contributes a quarter-wavelength resonant mode at about 1800 MHz to enhance the upper-band bandwidth of the antenna. In this study, the resonant modes contributed by the two shorted strips can be, respectively, adjusted by the length  $t$  in the longer shorted strip and the length  $d$  in the shorter shorted strip. Further, the patch monopole contributes a resonant mode to form a wide upper band of bandwidth larger than 1 GHz for the antenna to cover the GSM1800/1900/UMTS/LTE2300/2500 (1710–2690 MHz) operation. Also, the patch monopole uses a two-branch feeding design [19], which improves the impedance matching for its excited resonant mode.

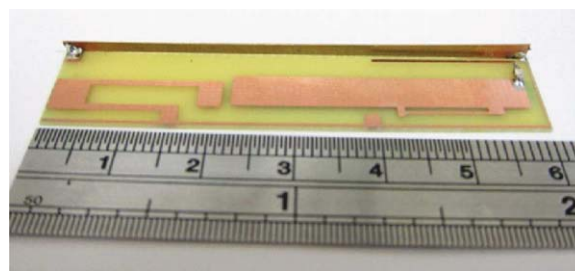
Note that the resonant mode in the desired lower band contributed by the longer shorted strip shows a single resonance and provide an operating bandwidth far from covering the antenna's desired lower band (704–960 MHz, bandwidth about 256

MHz or 31%). By embedding a chip-inductor-loaded narrow strip of length about 20.5 mm in-between the patch monopole and the longer shorted strip, the single-resonance mode in the antenna's lower band can become a dual-resonance mode, which makes the lower-band bandwidth greatly enhanced to cover the LTE700/GSM850/900 operation. This effect is owing to an equivalent parallel resonant circuit obtained, because the front terminal of the narrow strip is connected to the patch monopole and its end section is coupled to the longer shorted strip through a coupling gap of 0.7 mm. Also, the narrow strip is loaded with a chip inductor of 22 nH, and the chip-inductor-loaded narrow strip provides an equivalent inductance [20–22]. The coupling between the narrow strip and the longer shorted strip provides an equivalent capacitance [23–25]. The equivalent inductance and capacitance leads to the generation of a parallel resonance that is controllable by varying the inductance  $L$  of the chip inductor. In the proposed design, the parallel resonance is adjusted to be at the high-frequency tail of the single-resonance mode contributed by the longer shorted strip in the antenna's lower band. This parallel resonance leads to the generation of an additional resonance (zero reactance) at a frequency near the resonant frequency of the single-resonance mode, thereby resulting in a dual-resonance mode excited at about 900 MHz. Hence, a wide lower band for the antenna to cover the LTE700/GSM850/900 operation is obtained. Details of the results are discussed in Section 3 with the aid of Figure 5.

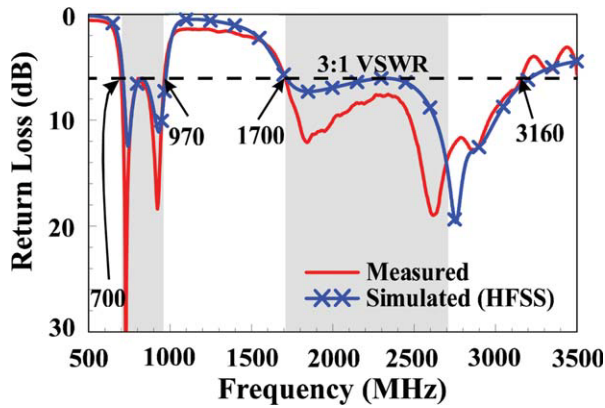
### 3. RESULTS OF FABRICATED ANTENNA

Figure 3 shows the measured and simulated return loss of the fabricated antenna (photo shown in Fig. 2). Note that the antenna is tested with the presence of the display ground shown in Figure 1. Measured results agree with the simulated results obtained using the three-dimensional (3D) full-wave electromagnetic field simulator HFSS [26]. Based on 3:1 VSWR or 6-dB return loss, which is widely used as the design specification of the internal WWAN mobile device antenna [27, 28], the obtained lower band and upper band can, respectively, cover the 704–960 and 1710–2690 MHz bands for eight-band WWAN/LTE operation.

To analyze the excited resonant modes of the antenna, Figure 4 shows the simulated return loss for the proposed antenna, Ref1 (the patch monopole with one feeding strip only), Ref2 (the patch monopole with two feeding strips), Ref3 (the patch monopole and the shorted longer strip only), and Ref4 (the patch monopole and two shorted strips only). In Figure 4(a), results for the proposed antenna, Ref1 and Ref2 are presented. Results show that the two-branch feeding strip indeed can lead to improved impedance matching of the excited resonant mode at about 2900 MHz contributed by the patch monopole. In Figure 4(b), results for the proposed antenna, Ref3 and Ref4 are



**Figure 2** Photo of the fabricated antenna. [Color figure can be viewed in the online issue, which is available at [wileyonlinelibrary.com](http://wileyonlinelibrary.com)]



**Figure 3** Measured and simulated return loss of the proposed antenna. [Color figure can be viewed in the online issue, which is available at [wileyonlinelibrary.com](http://wileyonlinelibrary.com)]

presented. By adding the longer shorted strip, a single-resonance mode at about 800 MHz and a resonant mode at about 2700 MHz are seen to be generated. Although by adding the shorter shorted strip, a resonant mode at about 1800 MHz is excited, which combines with the resonant modes at about 2700 and 2900 MHz, respectively, by the longer shorted strip and patch monopole to form the wide upper band for the antenna.

To study the effect of the excited parallel resonance in the proposed antenna, Figure 5 shows the simulated input impedance as a function of the inductance  $L$  of the chip inductor embedded in the parallel resonant circuit. Results for the inductance  $L$  varied from 0 to 22 nH are shown. The case of  $L = 0$  indicates that the chip inductor is not present and the narrow strip is directly connected to the patch monopole. Results clearly show that by varying the inductance of the loaded chip inductor,

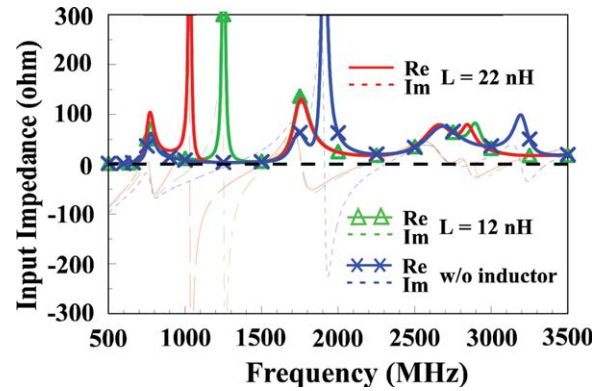


**Figure 5** Simulated input impedance as a function of the inductance  $L$  of the chip inductor embedded in the parallel resonant circuit. [Color figure can be viewed in the online issue, which is available at [wileyonlinelibrary.com](http://wileyonlinelibrary.com)]

the excited parallel resonance can be controlled and lead to the generation of an additional resonance near the resonant frequency of the existing single-resonance mode at about 800 MHz. In the proposed design, the preferred inductance  $L$  is 22 nH, and the additional resonance is at about 900 MHz. A dual-resonance is hence obtained in the desired antenna's lower band to achieve a much wider bandwidth. Also note that the chip inductor can also serve as a RF choker in the desired upper band owing to its large inductance at higher frequencies [29]. In this case, the added narrow strip will not affect the antenna performances in the desired upper band.

Figure 6 shows the measured antenna efficiency of the proposed antenna. The antenna efficiency is measured in a far-field anechoic chamber, and the mismatching loss is included in the measured results. The measured antenna efficiency is seen to be in the range of about 50–60% and 60–72%, respectively, in the antenna's lower and upper bands, which are acceptable for practical applications (generally required to be at least about 50%). The measured 3D total-power radiation patterns are plotted in Figure 7. The full 3D patterns and half 3D patterns with the cross-sectional cut at the  $x$ - $z$  plane at five representative frequencies in the antenna's lower and upper bands are shown. There are generally no nulls seen in the radiation patterns,

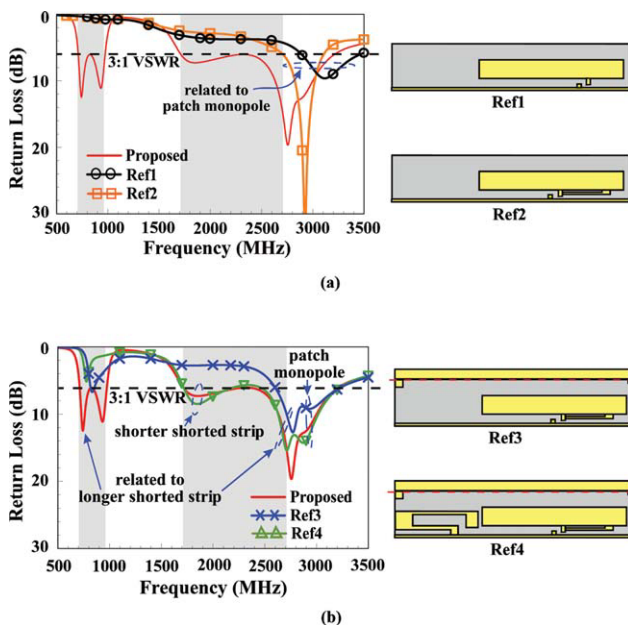


**Figure 4** (a) Simulated return loss for the proposed antenna, Ref1 (the patch monopole with one feeding strip only) and Ref2 (the patch monopole with two feeding strips). (b) Simulated return loss for the proposed antenna, Ref3 (the patch monopole and the shorter longer strip only) and Ref4 (the patch monopole and two shorter strips only). [Color figure can be viewed in the online issue, which is available at [wileyonlinelibrary.com](http://wileyonlinelibrary.com)]

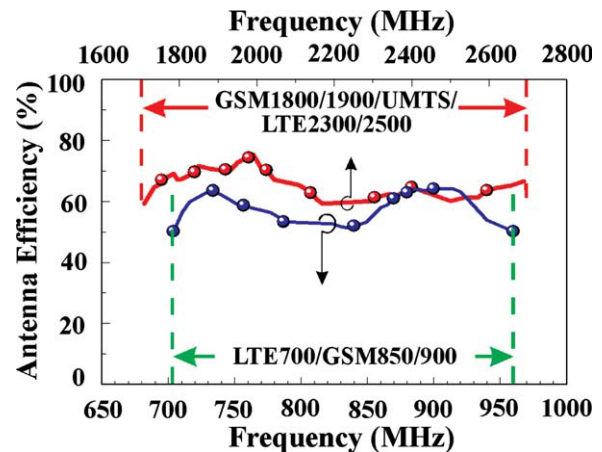


**Figure 6** Measured antenna efficiency (mismatching loss included) of the proposed antenna. [Color figure can be viewed in the online issue, which is available at [wileyonlinelibrary.com](http://wileyonlinelibrary.com)]



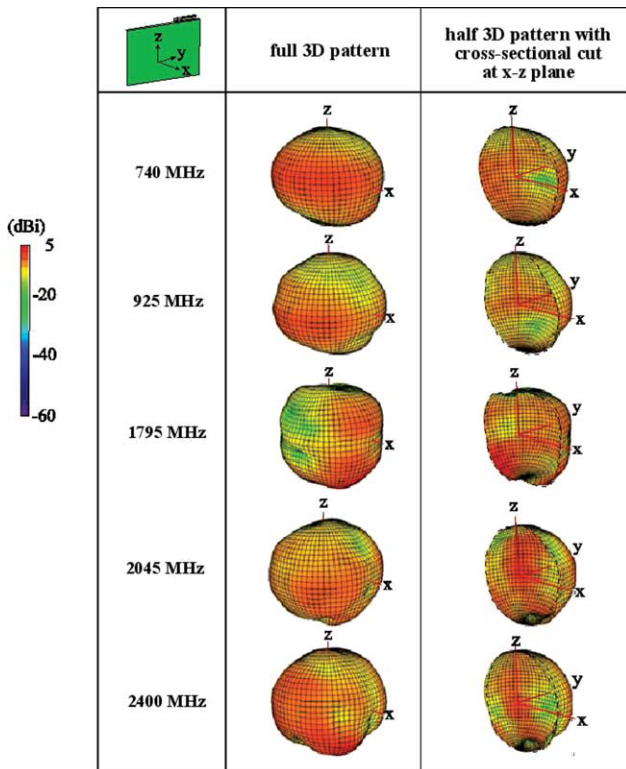


**Figure 7** Measured 3D total-power radiation patterns of the proposed antenna. [Color figure can be viewed in the online issue, which is available at [wileyonlinelibrary.com](http://wileyonlinelibrary.com)]

allowing no communication nulls expected in the practical applications.

#### 4. PARAMETRIC STUDY

Some design dimensions are also analyzed. Figure 8 shows the simulated return loss as a function of the length  $t$  in the longer shorted strip. Other parameters are the same as in Figure 1. Results for the length  $t$  varied from 50 to 60 mm are presented. Large effects are seen in the resonant modes related to the longer shorted strip, whereas the effects on the resonant modes related to the shorter shorted strip and patch monopole are relatively small. This also confirms the results analyzed in Figure 4,

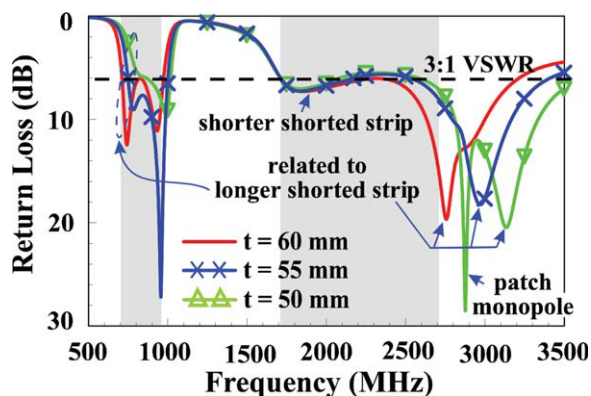


**Figure 8** Simulated return loss as a function of the length  $t$  in the longer shorted strip. Other parameters are the same as in Fig. 1. [Color figure can be viewed in the online issue, which is available at [wileyonlinelibrary.com](http://wileyonlinelibrary.com)]

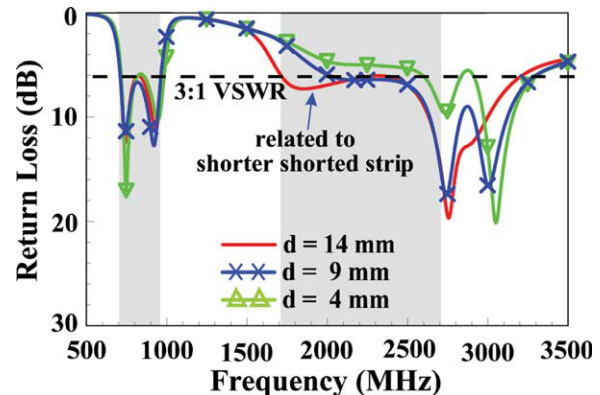


**Figure 9** Simulated return loss as a function of the length  $d$  in the shorter shorted strip. Other parameters are the same as in Figure 1. [Color figure can be viewed in the online issue, which is available at [wileyonlinelibrary.com](http://wileyonlinelibrary.com)]

and by varying the length  $t$ , the resonant modes at about 800 and 2700 MHz contributed by the longer shorted strip can be controlled.

Effects of the length  $d$  in the shorter shorted strip are also analyzed. Figure 9 shows the simulated return loss for the length  $d$  varied from 4 to 14 mm. As the variations in the length  $d$  also leads to the variations in the resonant length of the shorter shorted strip, the resonant mode contributed by the shorter shorted strip is greatly affected. When the length  $d$  decreases, the resonant mode contributed by the shorter shorted strip is shifted to higher frequencies, and the impedance matching is also greatly affected. Also, when the length  $d$  decreases, the degradation in the impedance matching of the excited resonant mode related to the shorter shorted strip also causes some effects on the resonant modes at about 2700 and 2900 MHz contributed, respectively, by the longer shorted strip and patch monopole. Properly selection of the length  $d$  in the shorter shorted strip is hence important in achieving the wide upper band for the proposed design.

#### 5. CONCLUSIONS

A WWAN/LTE tablet computer antenna with a small size of  $12 \times 60 \times 3.8 \text{ mm}^3$  has been reported. In the proposed antenna, the technique of using an embedded parallel resonant circuit in widening the lower-band bandwidth without increasing the antenna size has been applied. Operating principle of the parallel resonant circuit in widening the bandwidth has been addressed. Good radiation characteristics for frequencies over the antenna's lower and upper bands have also been observed. From the obtained results, the proposed antenna is promising for practical applications.

#### REFERENCES

1. X. Wang, W. Chen, and Z. Feng, Multiband antenna with parasitic branches for laptop applications, *Electron Lett* 43 (2007), 1012–1013.
2. C.H. Chang and K.L. Wong, Internal coupled-fed shorted monopole antenna for GSM850/900/1800/1900/UMTS operation in the laptop computer, *IEEE Trans Antennas Propag* 56 (2008), 3600–3604.
3. K.L. Wong and L.C. Lee, Multiband printed monopole slot antenna for WWAN operation in the laptop computer, *IEEE Trans Antennas Propag* 57 (2009), 324–330.
4. C. Zhang, S. Yang, S. El-Ghazaly, A.E. Fathy, and V.K. Nair, A low-profile branched monopole laptop reconfigurable multiband

- antenna for wireless applications, *IEEE Antennas Wireless Propag Lett* 8 (2009), 216–219.
5. C.W. Chiu, Y.J. Chi, and S.M. Deng, An internal multiband antenna for WLAN and WWAN applications, *Microwave Opt Technol Lett* 51 (2009), 1803–1807.
  6. K.L. Wong and S.J. Liao, Uniplanar coupled-fed printed PIFA for WWAN operation in the laptop computer, *Microwave Opt Technol Lett* 51 (2009), 549–554.
  7. K.L. Wong and F.H. Chu, Internal planar WWAN laptop computer antenna using monopole slot elements, *Microwave Opt Technol Lett* 51 (2009), 1274–1279.
  8. C.T. Lee and K.L. Wong, Study of a uniplanar printed internal WWAN laptop computer antenna including user's hand effects, *Microwave Opt Technol Lett* 51 (2009), 2341–2346.
  9. K.L. Wong, W.J. Chen, L.C. Chou, and M.R. Hsu, Bandwidth enhancement of the small-size internal laptop computer antenna using a parasitic open slot for the penta-band WWAN operation, *IEEE Trans Antennas Propag* 58 (2010), 3431–3435.
  10. T.W. Kang, K.L. Wong, L.C. Chou, and M.R. Hsu, Coupled-fed shorted monopole with a radiating feed structure for eight-band LTE/WWAN operation in the laptop computer, *IEEE Trans Antennas Propag* 59 (2011), 674–679.
  11. K.L. Wong, W.J. Chen, and T.W. Kang, Small-size loop antenna with a parasitic shorted strip monopole for internal WWAN notebook computer antenna, *IEEE Trans Antennas Propag* 59 (2011), 1733–1738.
  12. P. Vainikainen, J. Ollikainen, O. Kivekas, and I. Kelder, Resonator-based analysis of the combination of mobile handset and chassis, *IEEE Trans Antennas Propag* 50 (2002), 1433–1444.
  13. T.Y. Wu and K.L. Wong, On the impedance bandwidth of a planar inverted-F antenna for mobile handsets, *Microwave Opt Technol Lett* 32 (2002), 249–251.
  14. T.W. Kang and K.L. Wong, Internal printed loop/monopole combo antenna for LTE/GSM/UMTS operation in the laptop computer, *Microwave Opt Technol Lett* 52 (2010), 1673–1678.
  15. K.L. Wong and P.J. Ma, Coupled-fed loop antenna with branch radiators for internal LTE/WWAN laptop computer antenna, *Microwave Opt Technol Lett* 52 (2010), 2662–2667.
  16. T.W. Kang and K.L. Wong, Simple two-strip monopole with a parasitic shorted strip for internal eight-band LTE/WWAN laptop computer antenna, *Microwave Opt Technol Lett* 53 (2011), 706–712.
  17. Y.W. Chi and K.L. Wong, Very-small-size folded loop antenna with a band-stop matching circuit for WWAN operation in the mobile phone, *Microwave Opt Technol Lett* 51 (2009), 808–814.
  18. T.W. Kang and K.L. Wong, Isolation improvement of 2.4/5.2/5.8 GHz WLAN internal laptop computer antennas using dual-band strip resonator as a wavetraps, *Microwave Opt Technol Lett* 52 (2010), 58–64.
  19. K.L. Wong, C.H. Wu, and S.W. Su, Ultra-wideband square planar metal-plate monopole antenna with a trident-shaped feeding strip, *IEEE Trans Antennas Propag* 53 (2005), 1262–1269.
  20. C.H. Chang and K.L. Wong, Small-size printed monopole with a printed distributed inductor for penta-band WWAN mobile phone application, *Microwave Opt Technol Lett* 51 (2009), 2903–2908.
  21. C.T. Lee and K.L. Wong, Planar monopole with a coupling feed and an inductive shorting strip for LTE/GSM/UMTS operation in the mobile phone, *IEEE Trans Antennas Propag* 58 (2010), 2479–2483.
  22. Y.W. Chi and K.L. Wong, Quarter-wavelength printed loop antenna with an internal printed matching circuit for GSM/DCS/PCS/UMTS operation in the mobile phone, *IEEE Trans Antennas Propag* 57 (2009), 2541–2547.
  23. C.H. Chang and K.L. Wong, Printed  $\lambda/8$ -PIFA for penta-band WWAN operation in the mobile phone, *IEEE Trans Antennas Propag* 57 (2009), 1373–1381.
  24. K.L. Wong, W.Y. Chen, C.Y. Wu, and W.Y. Li, Small-size internal eight-band LTE/WWAN mobile phone antenna with internal distributed LC matching circuit, *Microwave Opt Technol Lett* 52 (2010), 2244–2250.
  25. K.L. Wong, W.Y. Chen, and T.W. Kang, On-board printed coupled-fed loop antenna in close proximity to the surrounding ground plane for penta-band WWAN mobile phone, *IEEE Trans Antennas Propag* 59 (2011), 751–757.
  26. <http://www.ansys.com/products/hf/hfss/>, ANSYS HFSS, Pittsburgh, PA.
  27. C.L. Liu, Y.F. Lin, C.M. Liang, S.C. Pan, and H.M. Chen, Miniature internal penta-band monopole antenna for mobile phones, *IEEE Trans Antennas Propag* 58 (2010), 1008–1011.
  28. S.J. Kim, K.H. Kong, M.J. Park, Y.S. Chung, and B. Lee, Design concept of a mobile handset to mitigate user's hand effect, *Microwave Opt Technol Lett* 50 (2008), 2696–2698.
  29. K.L. Wong, M.F. Tu, C.Y. Wu, and W.Y. Li, On-board 7-band WWAN/LTE antenna with small size and compact integration with nearby ground plane in the mobile phone, *Microwave Opt Technol Lett* 52 (2010), 2847–2853.

© 2011 Wiley Periodicals, Inc.

## SINGLE-/MULTIBAND CMOS LOW-NOISE AMPLIFIER USING CONCENTRIC SWITCHING INDUCTORS

Ruey-Lue Wang,<sup>1</sup> Shih-Chih Chen,<sup>2</sup> and Cheng-Lin Huang<sup>2</sup>

<sup>1</sup>Department of Electronic Engineering, National Kaohsiung Normal University, No.62, Shengjhong Rd., Yanchao Township, Kaohsiung County 824, Taiwan, Republic of china

<sup>2</sup>Graduate School of Optoelectronics, National Yunlin University of Science & Technology, Taiwan; Corresponding author: rlwang@nknpu.edu.tw

Received 7 May 2011

**ABSTRACT:** In this article, a low-noise amplifier (LNA) using concentric switching inductors were designed and measured. A voltage supply is fed through the switching inductors. The presented circuit is a modified cascoded amplifier configuration which input stage is a common-gate structure. The switching inductors are implemented by three series-wound concentric planar spiral inductors associated with two PMOSFET switches. According to on or off state of two PMOSFET switches, the circuit has theoretically four transfer characteristics, including one single-band, two dual-band, and one triple-band frequency responses. For the LNA, using the concentric-type switching inductors, the simulated and measured gains are nearly more than 12 and 10 dB at all operation frequency bands, respectively. The measured reflection coefficients are almost less than  $-10$  dB at all operation frequency bands. The measured minimum noise figures are almost less than 4.5 dB at all operation frequency bands. The power consumption is 9 mW. The chip size is  $1.03 \times 1.04$  mm<sup>2</sup>. © 2011 Wiley Periodicals, Inc. *Microwave Opt Technol Lett* 54:309–315, 2012; View this article online at [wileyonlinelibrary.com](http://wileyonlinelibrary.com). DOI 10.1002/mop.26591

**Key words:** low-noise amplifier; multiband; concentric-type switching inductors; LC resonance

### 1. INTRODUCTION

In recent years, many communication standards, such as worldwide interoperability for microwave access, wireless local area network, long-term evolution, and so on, have widely been used. In general, a modern wireless system is requested to provide multistandard or multiband operation [1]. Hence, front-end devices tend to be able to cohere with multistandard and multiband applications.

There are several ways of implementing a multiband or multistandard low-noise amplifier (LNA) [2–8]. A multiband or multistandard LNA circuit can be implemented by using a separate LNA for each frequency band, or directly designing a wide-band LNA without or with embedded notch filters [2, 3, 6], or designing a concurrent dual-band or multiband LNA [4, 5], or